3.4 AN IMPROVED ALGORITHM FOR ATMOSPHERIC WIND RETRIEVALS FROM SATELLITE SOUNDINGS OVER THE POLAR REGION

Cheng-Zhi Zou[1,2] and Weizhong Zheng[2,3]

[1]*NOAA/NESDIS/Office of Research and Applications, Camp Springs, Maryland*

[2]*Joint Center for Satellite Data Assimilation, Camp Springs, Maryland*

[3]*QSS Group, Inc., Lanham, Maryland*

1. Introduction

Recently, Zou and Van Woert (2001, 2002) developed a variational thermal wind method to retrieve the atmospheric winds from satellite temperature and surface wind observations. In this method, the thermal wind derived from the satellite temperature retrievals is added to the surface wind field to obtain a first-guess, nonmass-conserved atmospheric wind profile. Then a Lagrange multiplier in a variational formalism is used to force the first-guess wind to conserve mass. They have demonstrated that the satellite-derived atmospheric general circulation from the TOVS Pathfinder A temperature profile (Susskind et al. 1997) plus a SSM/I-based surface wind field exhibits structure similar to the NCEP-NCAR and ECMWF reanalysis winds over the Southern Ocean. In addition, the satellite-derived wind profiles compare favorably with the radiosonde observations at Macquarie Island with an annual mean biases near 0.5 m sec^{-1} for the meridional component and 1 m sec^{-1} for the zonal component, respectively. Furthermore, Francis et al. (2004) used this variational thermal wind technique to retrieve upper-level winds over the Arctic Ocean from TOVS Pathfinder–P temperature retrievals and found that the satellite-derived winds compare fairly well with the radiosonde observations from SHEBA experiments. In their validations, the meridional wind biases are also close to zero, similar to the validations over the Macquarie Island. Due to these good validation results, Francis et al. (2004) generated a 23-years, TOVS-based, daily atmospheric wind dataset over the Arctic Ocean. Trend analyses of this wind dataset suggest that the wind variability is compatible in dynamics with other observations such as sea ice extent variations.

In Zou and Van Woert (2002) studies, however, the satellite wind retrieval scheme was designed only for the surface conditions with open flat oceans. Over the land areas, boundary friction is important so that the thermal wind approximation may not work well. In this study, we develop a new algorithm that includes a planetary boundary layer (PBL) parameterization in the satellite retrieval scheme. With this PBL parameterization, the new algorithm can retrieve atmospheric winds under both land and ocean surface conditions. The performance of the algorithm is assessed using radiosonde observations at 11 stations around the Antarctic coast.

Corresponding author address: Dr. Cheng-Zhi Zou, Office of Research and Applications, NOAA/NESDIS, NOAA Science Center, Room 711, 5200 Auth Road, Camp Springs, MD 20746
E-mail: cheng-zhi.zou@noaa.gov

2. Satellite wind retrieval algorithm

Over the middle and high latitudes, the nonlinear advection terms are of second order quantities in the momentum equations and, therefore, they can be ignored compared to other terms such as the geostrophic winds. With this approximation, the diagnostic equations for the mass conservation and momentum that include frictions are written as follows

$$\nabla \bullet \mathbf{V} + \frac{1}{\rho}\frac{\partial(\rho w)}{\partial z} = 0 , \tag{1}$$

$$f(v - v_g) = \frac{1}{\rho}\frac{\partial}{\partial z}(\rho \overline{u'w'}) , \tag{2}$$

$$f(u - u_g) = -\frac{1}{\rho}\frac{\partial}{\partial z}(\rho \overline{v'w'}) , \tag{3}$$

where u_g and v_g are the geostrophic zonal and meridional wind speeds, respectively. All other symbols assume their usual meteorological meanings and fluctuations in the density of air have been neglected.

The above equations comprise the foundations for the current satellite wind retrievals over the polar region. In order for the algorithm to be able to retrieve winds over the land and plateau areas with reasonable accuracy, a PBL model needs to be included in (1) through (3). With Holtslag and Boville's PBL scheme (1993), the surface fluxes are parameterized by

$$(\overline{u'w'})_0 = -C_M |V_1| u_1 , \tag{4}$$

$$(\overline{v'w'})_0 = -C_M |V_1| v_1 . \tag{5}$$

where V is a scalar wind speed; the subscripts 0 and 1 refer to values at the surface and at the reference level respectively; C_M is the surface layer exchange coefficient and is defined as

$$C_M = C_N f_M(R_b), \quad (6)$$

here C_N is the neutral exchange coefficient which is given by

$$C_N = \frac{k^2}{\ln((z_1 + z_{0M})/z_{0M})\ln((z_1 + z_{0M})/z_{0M})}, \quad (7)$$

k = 0.4 is the von Kármán constant, z_1 is the height of the reference level, and z_{0M} is the roughness length for momentum. The bulk Richardson number R_b is defined as

$$R_b = \frac{g z_1}{\theta_1} \frac{(\theta_1 - \theta_0)}{|V_1|^2}, \quad (8)$$

where g is the acceleration of gravity, θ_0 and θ_1 are the potential temperatures at the surface and the reference level, respectively. Under unstable conditions (R_b < 0), the function, f_M, that modifies the neutral-exchange coefficient is given by

$$f_M(R_b) = 1 - \frac{10R_b}{1 + 75C_N\{[(z_1 + z_{0M})/z_{0M})]\}|R_b|^{1/2}}, \quad (9)$$

while under stable conditions ($R_b \geq 0$), it is taken as

$$f_M(R_b) = \frac{1}{1 + 10R_b(1 + 8R_b)}. \quad (10)$$

Above the surface layer, the turbulent mixing is treated by a first-order local diffusion,

$$\rho\overline{u'w'} = -\rho K_M \frac{\partial u}{\partial z}, \quad (11)$$

$$\rho\overline{v'w'} = -\rho K_M \frac{\partial v}{\partial z}. \quad (12)$$

Here K_M denotes the momentum transfer coefficient due to turbulence and molecular effect. It is taken as a function of a length scale l_c and local vertical gradients of wind and potential temperature,

$$K_M = l_c^2 S F_c(R_i), \quad (13)$$

where S is the vertical wind shear and R_i is the Richardson number. Detailed specifications for these parameters are referred to Holtslag and Boville's (1993).

The wind retrieval procedure is described as follows. Given the surface pressure field and vertical temperature profiles, the surface geopotential height can be first computed using the hydrostatic balance equation, $\frac{\partial \psi}{\partial p} = -\frac{RT}{P}$, where Ψ is the geopotential height, and then the surface geostrophic wind can be obtained from the surface geopotential field. After the surface geostrophic wind is obtained, the vertical geostrophic wind profiles can be derived form the thermal wind equations,

$$\frac{\partial u_g}{\partial \ln p} = \frac{R_d}{f} \frac{\partial T}{a\partial\varphi}, \quad (14)$$

$$\frac{\partial v_g}{\partial \ln p} = -\frac{R_d}{f} \frac{\partial T}{a\cos\varphi\partial\lambda}. \quad (15)$$

With the geostrophic wind profiles being obtained and assuming the surface wind field is known (from satellite observations or analysis system), a first-guess wind filed can be solved from (2) and (3) plus the PBL parameterizations (4) through (13). Finally, a variational mass-conservation scheme from Zou and Van Woert (2002) is used to force the first-guess wind to conserve mass.

3. Data

We use surface pressure and surface wind fields from Global Data Assimilation System (GDAS) as known inputs for the satellite algorithm development. In addition, to understand the algorithm performance, we use the temperature profiles also from GDAS as inputs to the retrieval algorithm. This is because radiosonde observations have been assimilated into GDAS so that the errors in the retrieved winds near the radiosonde stations may solely come from the algorithm, not from the satellite temperature profiles that may have unknown errors over the plateau regions. After the accuracy of the retrieval algorithm is understood, the satellite-retrieved temperature profiles will then be used as inputs.

The GDAS data used in this study have a temporal resolution of 6 hours and horizontal spatial resolution of $1^0 \times 1^0$.

4. Results

Figure 1a-d show validations of the wind profiles derived from the current algorithm against radiosonde observations at 11 stations around the Antarctic coast for July 2002. Also shown in the figures are GDAS winds at the radiosonde locations for the same month. Figure 1 shows that, except at the Argentina's Base Marambio Station ($64^0$14'S, $56^0$43'W) at the tip of the Antarctic Peninsula, the derived winds exhibit similar directions as the radiosonde observations. At 850 mb at the Base Marambio Station, the GDAS and derived winds have similar wind directions but they are nearly opposite to the wind direction of the radiosonde observations. This large difference between GDAS and the radiosonde observations is unexpected.

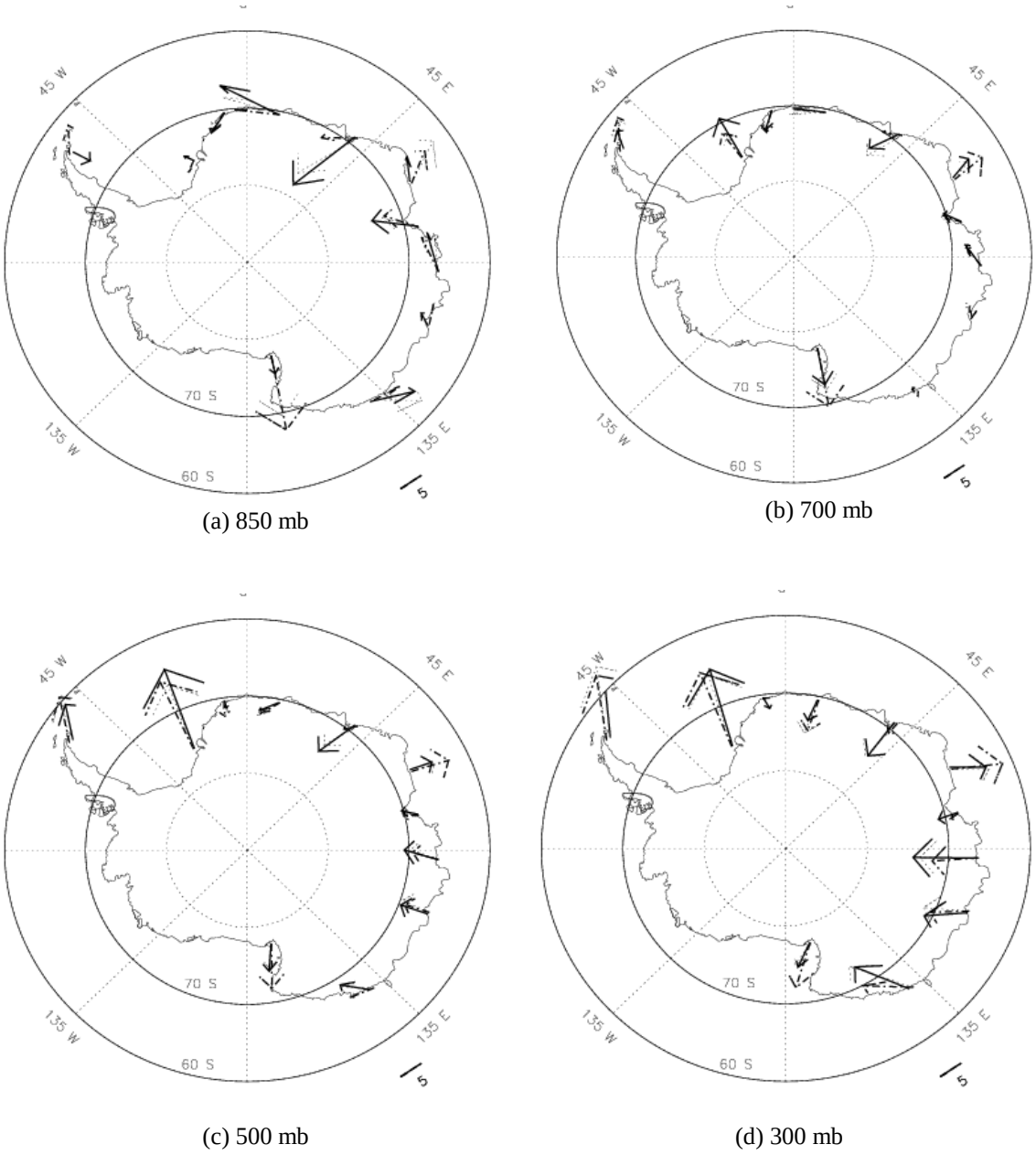

(a) 850 mb (b) 700 mb

(c) 500 mb (d) 300 mb

Fig. 1 Comparisons of the wind profiles derived from the satellite algorithm against radiosonde observations and GDAS for July 2002 monthly means. The thick solid line represents the radiosonde observations, the thin dashed lines are GDAS, and the dash-dotted lines are winds derived from the algorithm developed in this study. Note that the derived winds are the 'first-guess' winds where the mass conservation constraint is not applied yet in these figures. (a) 850 mb; (b) 700 mb; (c) 500 mb; and (d) 300 mb. Unit is m sec^{-1}.

It occurs probably because the quality control procedure in the GDAS system had thrown away most radiosonde observations when these observations yielded fundamental differences from the GDAS wind structure over this region. (See Figure 2). This situation occurs only at 850 mb at the Base Marambio Station. At other levels at the Base Marambio Station, both the GDAS and the derived winds yield similar directions as the radiosonde observations.

Figure 2a-f show comparisons between the derived monthly mean winds for July 2002 using the satellite algorithm and the corresponding GDAS winds over the Antarctic and Southern Ocean regions at 850 mb and 500 mb, respectively. At 850 mb, the derived winds and GDAS winds show very small differences over the ocean area and some land areas that do not have radiosonde observations, suggesting that the satellite algorithm has similar boundary dynamics as GDAS so

they produce a wind field with similar accuracy. Near the Antarctic coast, larger differences are observed between the derived and GDAS winds, especially near the locations where radiosonde observations have been assimilated into GDAS (see Fig. 1 for radiosonde locations). This basically suggests that the large differences between the derived and GDAS winds are mainly due to the differences between the derived winds and the radiosonde observations, assuming that GDAS winds faithfully represent the radiosonde winds where radiosonde data are being assimilated.

At 500 mb, the differences between the derived and GDAS winds are small over both oceans and the interior Antarctic continent. In addition, their differences near the Antarctic coast are much smaller compared to 850 mb. This is consistent with Fig. 1 that the differences between the derived winds and radiosonde observations are smaller at this level.

4. Conclusions

An algorithm for retrieving upper-level winds from satellite temperature retrievals over the polar plateau region is developed. Validations against radiosonde observations at 11 stations using the GDAS temperature as inputs show encouraging results. Future studies will focus on using AMSU and AIRS temperature retrievals as inputs to the satellite algorithm to test its performance.

Acknowledgement The GDAS data are taken from NOAA/NCEP and the radiosonde data are from NCDC. This study is supported by the NPOESS program of Integrated Program Office. The views, opinions, and findings contained in this report are those of the author(s) and should not be construed as an official National Oceanic and Atmospheric Administration or U.S. Government position, policy, or decision.

REFERENCES

Francis, J. A.,2002: Validation of reanalysis upper-level winds in the Arctic with independent rawinsonde data, *Geophys. Res. Let*., **29**, 1-4.

Francis, J. A., E. Hunter, and C.-Z. Zou, 2004: Arctic tropospheric winds derived from TOVS satellite retrievals, *J. Climate*, in press.

Holtslag, A. A. M., and B. A. Boville, 1993: Local versus nonlocal boundary-layer diffusion in a global climate model. *J. Climate*, **6**, 1825-1842.

Susskind, J, P. Piraino, L. Rokke, L. Iredell, and A. Mehta, 1997: Characteristics of the TOVS Path A dataset, *Bull. Amer. Metorol. Soc*., **78**. 1449-1472.

Zou, C.-Z., and M. Van Woert, 2001: The role of conservation of mass in the satellite-derived poleward moisture transport over the Southern Oceans. *J. Climate,* **14**, 997-1016.

Zou, C.-Z., and M. Van Woert, 2002: Atmospheric wind retrievals from satellite soundings over the middle and high latitude oceans, *Mon. Wea. Rev*., **130**, 1771-1791.

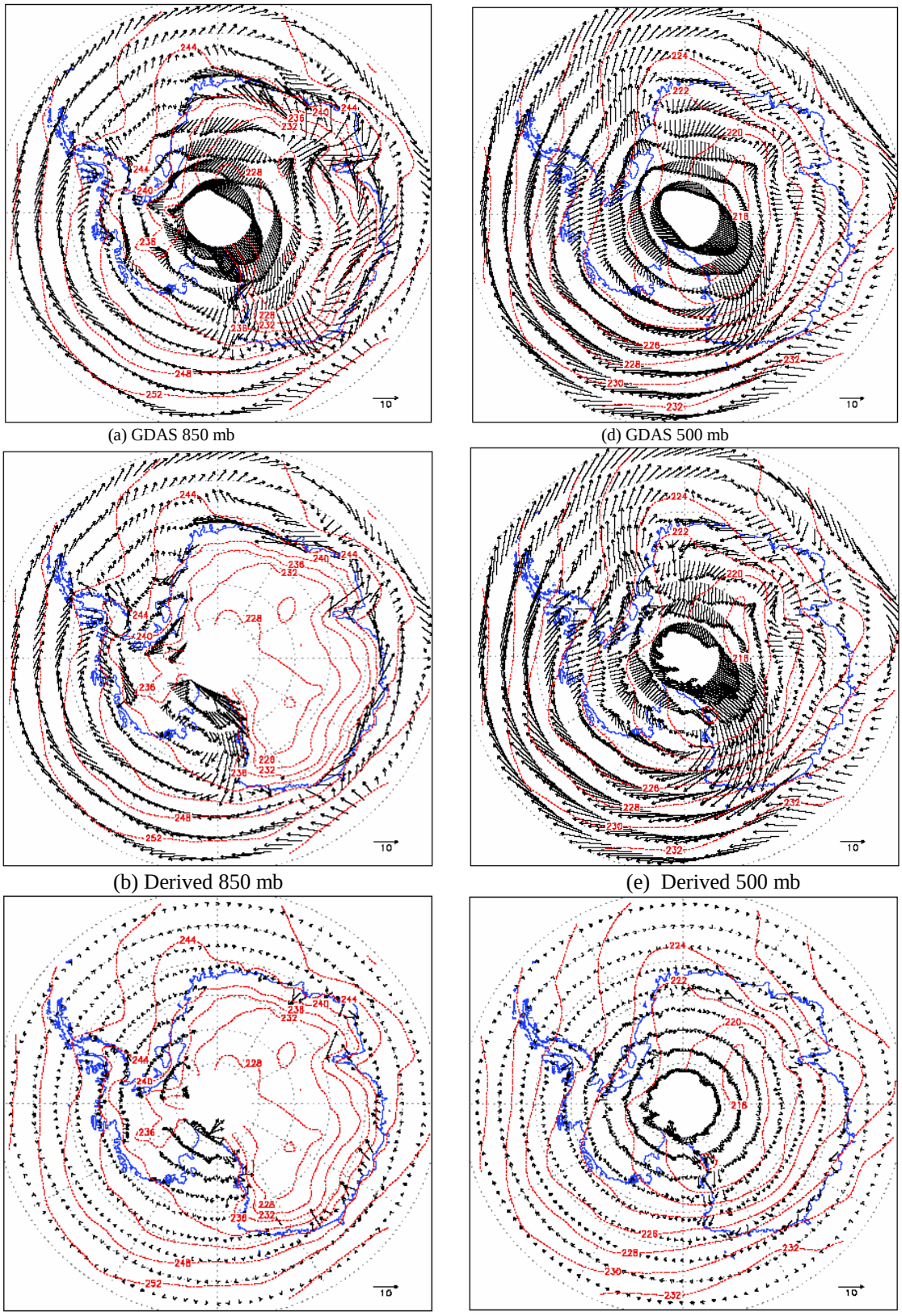

(a) GDAS 850 mb (d) GDAS 500 mb

(b) Derived 850 mb (e) Derived 500 mb

(c) [(b)-(a)] (f) [(e)-(d)]

Fig. 2 Comparisons of July 2002 monthly mean winds between GDAS and derived using newly developed algorithm.